

# Direct Numerical Simulations of Fundamental Turbulent Flows with the Largest Grid Numbers in the World and its Application of Modeling for Engineering Turbulent Flows

Group Representative

Chuichi Arakawa CCSE, Japan Atomic Energy Research Institute, Group Leader

Authors

Chuichi Arakawa CCSE, Japan Atomic Energy Research Institute, Group Leader

Yukio Kaneda School of Engineering, Nagoya University, Professor

Oliver Fleig School of Engineering, The University of Tokyo, Graduate Student

High-resolution direct numerical simulations (DNSs) of incompressible turbulence with the numbers of grid points up to  $4096^3$  were executed on the Earth Simulator (ES). The DNSs are based on a Fourier spectral method. In DNS based on the spectral method, most of the computation time is consumed in calculating the three-dimensional (3D) Fast Fourier Transform (FFT), which requires huge-scale global data transfer and has been the major stumbling block that has prevented truly high-performance computing. By implementing new methods to efficiently perform the 3D-FFT on the ES, we have achieved DNS at 16.4 Tflops on  $2048^3$  grid points. The DNS provides us with indispensable data for turbulence research. For example, the data shed light on fundamental questions, such as those on the turbulence energy spectrum, energy dissipation rate, intermittency, etc. The data analysis is now underway.

An engineering application is also performed. The aim is to simulate the aerodynamic noise emitted from wind turbine blade tips. The simulation of high frequency pressure fluctuations requires the smallest vortical structures in the flow to be resolved very accurately, which in turn requires a large number of grid points. The noise causing unsteady flow field around a wind turbine blade was analyzed using Large Eddy Simulation (LES). A simulation with 100 Million grid points was performed on the ES. LES gives us new insight into the physical phenomena causing tip vortex formation and tip noise.

**Keywords:** Turbulent flow, DNS, Kolmogorov scale, LES, blade, noise, tip vortex

## 1. High-resolution DNS of incompressible turbulence

Direct numerical simulation (DNS) of turbulent flows provides us with detailed turbulence data that are free from experimental ambiguities such as the effects of using Taylor's hypothesis, one dimensional surrogates, etc. However, the degrees of freedom or resolution necessary for DNS increases rapidly with the Reynolds number. The maximum resolution is obviously limited by the available computing memory and speed. The Earth Simulator (ES), with a peak performance and main memory of 40 TFlops and 10 TBytes, respectively, provides a new opportunity in this respect.

The problem of turbulence of an incompressible fluid obeying the Navier-Stokes equations under periodic boundary conditions is one of the most fundamental (canonical) problems in the study of turbulence by DNS. Its boundary conditions are simple, but it still keeps the essence of turbulence dynamics; the nonlinearity due to the convective effect

associated with the fluid motion, the dissipativity due to the viscosity and the non-locality due to the pressure. We call below such turbulence as "box turbulence". We performed DNSs of box turbulence by using an alias-free spectral method. Spectral methods have the advantage over conventional finite difference schemes in the sense that the incompressibility condition, or equivalently the mass conservation law, is rigorously satisfied by the methods. They have been in fact preferred because of its accuracy in the studies of canonical problems, but the resolution in the DNSs based on spectral methods has so far been limited up to  $1024^3$  grid points. Recently, we could achieve DNSs of box turbulence up to  $4096^3$  grid points on the ES. The DNSs provide us with indispensable data for turbulence research.

### 1.1. Optimization and performance of the DNS program

Since the three-dimensional (3D) Real Fast Fourier

Table 1 Performance in Tflops of the computations with double [single] precision arithmetic as counted by the hardware monitor on the ES. The numbers in ( - ) denote the values for computational efficiency. The number of APs in each PN is a fixed 8.

$Nn_n$	512	256	128	64
2048	13.7(0.43)[15.3(0.48)]	6.9(0.43)[7.8(0.49)]	-	-
1024	11.3(0.35)[11.2(0.35)]	6.2(0.39)[7.2(0.45)]	3.3(0.41)[3.7(0.47)]	1.7(0.43)[1.9(0.48)]
512	-	4.1(0.26)[4.0(0.25)]	2.7(0.34)[3.0(0.38)]	1.0(0.26)[1.1(0.28)]
256	-	-	1.3(0.16)[1.2(0.15)]	1.0(0.26)[1.1(0.28)]
128	-	-	-	0.3(0.07)[0.3(0.07)]

Transform (RFFT) accounts for more than 90% of the computational cost of executing the code for DNS of box turbulence by the Fourier spectral method, the most crucial factor in maintaining high levels of performance in the DNS of turbulence is the efficient execution of this calculation.

We achieved a high-performance 3D-RFFT by implementing the following ideas/methods on the ES. (See Ref.1 for the detail.)

- (1) Data Allocation: To perform the 3D-RFFT for  $N^3$  real-valued data, say  $u$ , we allocated the data to the global memory region (GMR) of a PN. The size of data set for  $u$  on each PN is  $(N+1) \times (N/n_d) \times N$ , while that of the real and imaginary part of the Fourier transform of  $u$  is  $(N+1) \times N \times (N/2 / n_d)$ . Here  $n_d$  is the number of PNs, the symbol  $n_i$  in  $n_1 \times n_2 \times n_3$  denotes the data length along the  $i$ -th axis, and we set the length along the first axis to  $(N+1)$ , so as to speed up the memory throughput by avoiding memory-bank conflict.
- (2) Parallelization by Microtasking: For efficiently performing the  $N \times (N/2 / n_d)$  1D-FFTs of length  $N$  along the first axis, the data along the second axis is divided up equally among the 8 APs of the given PN using the manual insertion of the parallelization directive "`*cdir parallel do`" before target do-loops.
- (3) Radix-4 FFT: Though the peak performance of an AP of the ES is 8 Gflops, the bandwidth between an AP and the memory system is 32 GB/s. This means that only one double-precision floating-point datum can be supplied for every two possible double-precision floating-point operations. This causes a bottleneck of memory access in the kernel loop of a radix-2 FFT and degrades the sustained levels of performance on the overall task. Thus, to efficiently calculate the 1D-FFT within the ES, the radix-4 FFT must replace the radix-2 FFT to the extent that this is possible.
- (4) Data Transposition by Remote Memory Access: Before performing the 1D-FFT along the 3rd axis, we need to make the data transposition in such way that the axis of domain decomposition can be changed from the 2nd to the 3rd axis. The remote memory access (RMA) function is used for transferring  $N \times (N/$

$n_d) \times (N/2 / n_d)$  data from each of the  $n_d$  PNs to the other PNs. The data transposition can be completed with  $(n_d - 1)$  such RMA-transfer operations, after which  $N \times (N/n_d) \times (N/2)$  data will have been stored at each target PN. The 1D-FFT for the 3rd axis is then executed.

We have measured the sustained performance for both the double-precision and single-precision versions of the DNS code by using a hardware counter in the ES. Table 1 shows the sustained performance in Tflops and the computational efficiency, in which we change the number  $N^3$  as  $N=128, 256, 512, 1024$ , and  $2048$ . The numbers of PNs used in these DNSs are 64, 128, 256, and 512. The maximum sustained performance of 15.3 Tflops, which corresponds to 48% of the peak performance, was achieved for the problem size of  $2048^3$  with 512 PNs [16.4 Tflops (again the maximum) was achieved for the same case, according to the evaluation based on the analytical expressions of the numbers of operations].

The CPU time of the ES for one time step of the Runge-Kutta-Gill method in single precision for the run with  $N=4096$  and  $n_d=512$  was 30.7 seconds. Simulations of this size are only practicable on the ES. We estimate that statistically steady state of the turbulence is obtained after at least two eddy-turn-over times  $2T$ , which costs over 16,000 time steps.

## 1.2. DNS results

All of the runs, except the one with  $N=4096$ , were performed with double-precision arithmetic and continued until the time  $t \sim 5T$ . Single-precision arithmetic was used in the run with  $N=4096$ , except for the 3D-RFFT, and this run was continued until  $t \sim 1.5T$ . The DNSs reveal aspects of turbulence, which have been missed in previous DNSs. Most importantly, the DNS data present inertial subrange of turbulence, which is much wider than any one so far realized by DNSs with lower resolutions. Such data can be used to get new insights or understanding on fundamental questions in turbulence research.

Among the fundamental questions is the one related to the well-known  $k^{-5/3}$  energy spectrum by Kolmogorov, where  $k$  is the wavenumber. The DNSs suggest that the energy spec-

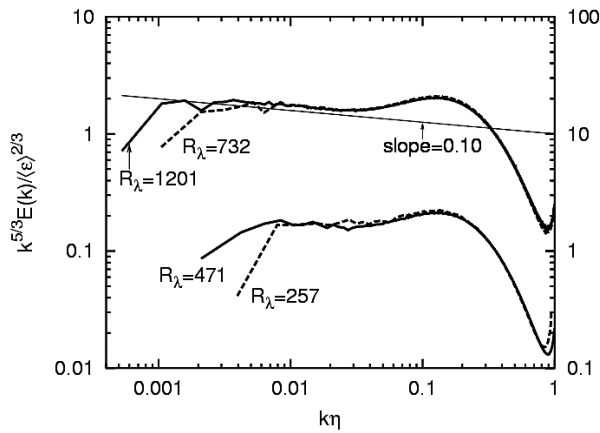


Fig. 1 Compensated energy spectra from DNSs with (A)  $N=512, 1024$ , and (B)  $N=2048, 4096$ . Scales on the right and left sides are for (A) and (B), respectively. (From Ref.2)

trum in the inertial subrange is fairly close to Kolmogorov's  $k^{-5/3}$  spectrum. However, the DNSs at the same time show that the exponent is slightly different from  $-5/3$ , unexpectedly from DNSs with low resolutions. (See Fig.1.) Another fundamental question is on the energy dissipation rate in the limit of high Reynolds number  $Re$ . The independence of normalized energy dissipation rate  $D$  has been the basic premise in phenomenology of turbulence and its significance has been well recognized. Our DNSs demonstrate that  $D$  tends to a constant independent of  $Re$ , as  $Re$  tends to infinity. (See Ref.2 for the detail.)

The statistics of the dissipation rate  $\epsilon$  per unit mass plays the key role in many turbulence theories including those by Kolmogorov. The statistics of the enstrophy  $\omega^2$  and pressure  $p$  is also the key ingredients of turbulence theories. One of the simplest and fundamental measures characterizing the statistics of these quantities is the spectrum of their squares. By analyzing the DNS data, we found that there exists a wave number range (inertial subrange) in which the spectra scale with the wave number  $k$  like  $k^a$ . Exponent  $a$  for  $p$  is about 1.81, which is in good agreement with the value obtained by assuming the joint probability distribution of the velocity field to be Gaussian, while  $a$  values for  $\epsilon$  and  $\omega^2$  are about  $2/3$ , and very different from the Gaussian approximation values. (See Ref.3 for the detail.)

This report was written on the basis of Refs 1-3. The readers may refer them for the details.

## 2. Simulation of tip vortex flow and tip noise of a blade using Large Eddy Simulation

An application for modeling of engineering turbulent flow was also performed as part of this project. The aim is to simulate the tip vortex flow and its associated tip noise emitted from rotating blade tips.

The shape of the blade tip has a considerable effect on the

tip noise and thus the overall noise. Blade tip shapes optimized for reduced noise emission would allow a wind turbine to operate at optimum tip speed ratio with increased energy capture. In this work a blade with finite span is analyzed using Large Eddy Simulation.

### 2.1. Computational methods

Aerodynamic noise is caused by the pressure fluctuations in the flow. Time averaged simulation is the most commonly used tool for flow simulation in engineering applications. However, this method cannot provide time accurate information of the pressure fluctuations. LES (Large Eddy Simulation) is a very promising tool for aeroacoustics as it can simulate in a time accurate way the small vortical structures in the flow. It is able to predict turbulent frequency spectra and the noise generating mechanisms. However, it requires a large number of computational grid points to resolve the smallest length scales. An LES code has been developed and optimized for the Earth Simulator to analyze the unsteady flow field and noise sources of rotating wind turbine blades of arbitrary shape and to estimate their acoustic emissions. In the present work the unsteady fluctuations around a stationary finite wind turbine blade in an incident flow is analyzed using compressible LES. The Reynolds number is 200,000, the Mach number 0.3 and the angle of attack is 4 degrees. Figure 2 shows the computational grid. The blade is of airfoil section MEL012, a typical wind turbine airfoil. The grid consists of 255 points in the chordwise direction, 129 points normal to the blade surface and 3040 points in the spanwise direction. The total number of grid points is approximately 100 Million. The computational mesh in the tip region of the blade is made extremely fine in the spanwise direction ( $5 \times 10^{-4}$  of the chord length) to accurately simulate the tip vortex and to resolve the noise causing high frequency pressure fluctuations inside the tip vortex. The simulation was performed on 10 nodes. It takes about 3.8 CPU hours per processor to achieve a regular fluctuation state.

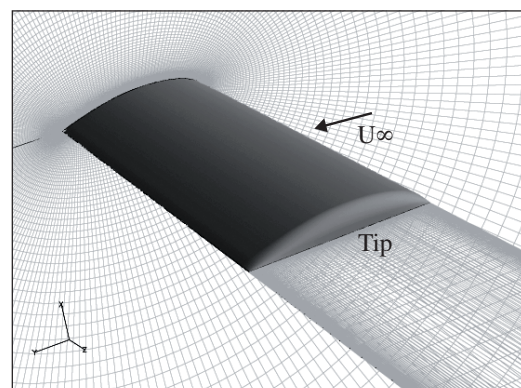


Fig. 2 Computational grid - MEL012 blade

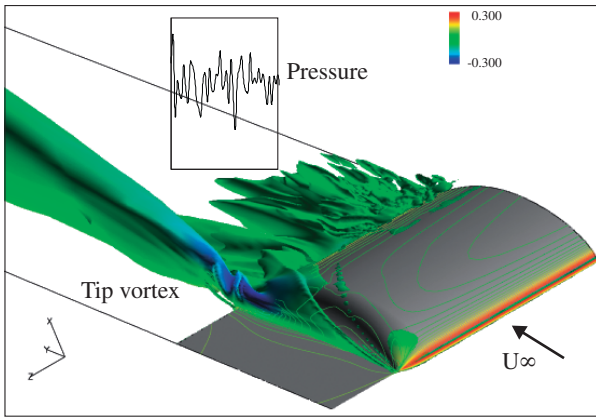


Fig. 3 Vorticity  $\omega_x$  Isosurfaces (Color denotes pressure)

## 2.2. Results

The simulation succeeded in capturing the unsteady laminar separation bubble and turbulent reattachment phenomena. The surface pressure distribution obtained by LES agrees reasonably well with experimental measurements. The turbulent tip vortex and vortical structures in the tip region can be identified in Fig. 3. Time accurate pressure fluctuations inside the tip vortex have been obtained by LES. This would not have been possible using the usual time-averaging flow simulation. The turbulent flow in the tip vortex is convected inboard and aft towards the trailing edge. The cross flow

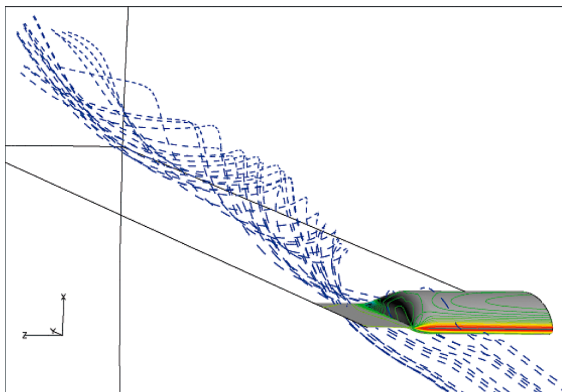


Fig. 4 Particle tracks around tip vortex

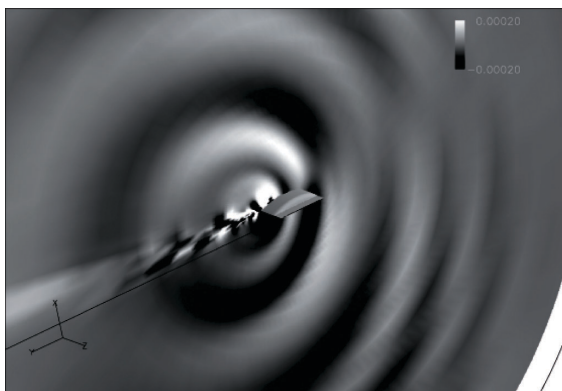


Fig. 5 Instantaneous acoustic pressure perturbation field

over the blade tip is responsible for the formation of the tip vortex. Tip noise is thought to be caused by the interaction of the tip vortex with the trailing edge and by turbulence in the locally separated flow region associated with the formation of the cross flow around the tip edge. Tip vortex noise is of broadband character and is influenced by the spanwise extent of the vortex. Further simulations of the blade tip will be performed to fully understand the origin of tip noise. Figure 4 shows the particle tracks behind the blade. The structure of the tip vortex can be seen. The broadband aerodynamic noise perceived in the far-field is caused by the fluctuations inside the tip vortex and by the fluctuations generated when the tip vortex collides with the blade. It is predicted by simulating the propagation of the pressure fluctuations using LES in the near field and Kirchhoff's integral method in the far-field, as seen in Fig. 5. Here, the pressure perturbations also contain contributions from the fluctuations generated by the laminar separation bubble. Concerning large and fast rotating wind turbines, the contribution by tip vortex fluctuations will be much more pronounced than separation related noise due to lower angles of attack and higher speeds in the tip region.

In the next stage of this project, a parametric study with different tip shapes will be performed and the effect of the tip shape on the broadband noise examined with the aim of selecting those that produce the lowest acoustic emissions. Rotational effects will be included. The tip shape shown in Fig. 6 has been shown in field tests to reduce acoustic emissions of wind turbines. It is presently being simulated on Earth Simulator. Due to the thin extension a strong leading edge wake is expected to build up and possibly being able to disturb the generation of the tip wake. It would be ideal to design a blade tip shape that reduces the interaction of the turbulent vortex core with the trailing edge. It is hoped that the design of optimized tip shapes will lead to reduced noise emission of future large and fast rotating wind turbines and to improved public acceptance of wind energy. LES at higher Reynolds numbers will be performed in the future. It is

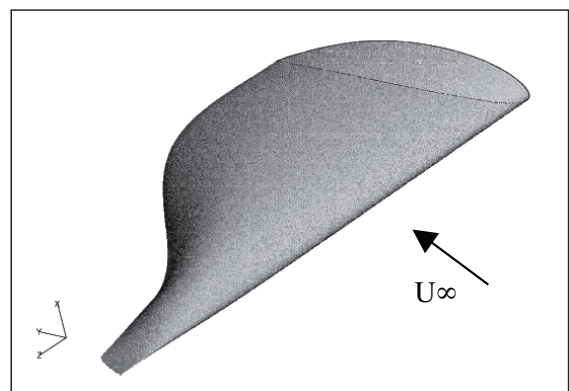


Fig. 6 Future tip shape

estimated that 3-4 Billion grid points would be required for accurate simulation of a blade tip at high Reynolds numbers in order to capture the transition from laminar to turbulent flow near the leading edge. This would require 100 nodes on the Earth Simulator and would be a world record in the number of grid points used for the simulation of a blade.

### 2.3. Optimization

The current parallel efficiency using 240 Million grid points is 99.99%. Vectorization ratio is 99.3% with an average vector length of 253. All repetitive loops are fully vectorized. MPI is used for inter-nodal and inter-processor data exchange. Optimized speed-up is achieved by making the inner loop long for optimal vectorization and by parallelizing the outer loop. The domain is split along the blade axis only.

### References

1. Mitsuo Yokokawa, Ken'ichi Itakura, Atsuya Uno, Takashi Ishihara and Yukio Kaneda: Proc. the IEEE/ACM SC2002 Conference, Baltimore, 2002, <http://www.sc-2002.org/paperpdfs/pap.pap273.pdf>.
2. Yukio Kaneda, Takashi Ishihara, Mitsuo Yokokawa, Ken'ichi Itakura, and Atsuya Uno: *Physics of Fluids*, **15** no.2 L21-L24 (2003).
3. Takashi Ishihara, Yukio Kaneda, Mitsuo Yokokawa, Ken'ichi Itakura, and Atsuya Uno: *J. Phys. Soc. Jpn.*, **72** no.5 (2003) (*to appear*).
4. Wagner, S., Bareis, R., Guidati, G.: *Wind turbine noise*, Springer-Verlag, Berlin, Germany (1996).



## 乱流の世界最大規模直接数値計算とモデリングによる応用計算

利用責任者

荒川 忠一 日本原子力研究所 計算科学技術推進センター 並列計算法開発グループ グループリーダー

著者

荒川 忠一 日本原子力研究所 計算科学技術推進センター 並列計算法開発グループ グループリーダー

金田 行雄 名古屋大学大学院 工学研究科 計算理工学専攻 教授

地球シミュレータ(ES)上で格子点総数が最大4096<sup>3</sup>に及ぶ、スペクトル法に基づく世界最大規模の非圧縮性乱流の直接数値シミュレーション(DNS)を行った。スペクトル法に基づくDNSでは計算時間の大部分が高速フーリエ変換(FFT)の実行に費やされるため、FFTの効率化がDNSの高効率化のためにきわめて重要である。我々はその効率化のための新手法を開発、実装してES上で16.4TflopsのDNS(格子点数2048<sup>3</sup>)を実現した。そのDNSは乱流研究のための貴重なデータベースを提供する。そのデータ解析は現在進行中であるが、すでにこれまでエネルギースペクトルについての新しい知見など、いくつかの成果が得られている。

具体的には、一様減衰乱流を対象に、テラー長に基づくレイノルズ数が1217に達するシミュレーションを実行した。この値は通常の室内実験の規模を上回るものであり、図1は渦度の等値面によって乱流渦構造を示したものである。一方、レイノルズ数の増大に伴い、コルモゴロフの実験値からのわずかなずれも観察された。

応用計算に関しては翼周りの流れの格子1億点における大規模並列LES(Large-Eddy-Simulation)計算を行った。翼の回転に伴う翼端渦の解明と空力騒音の高精度予測を目指し、翼スパン方向に翼弦長方向と同等の格子点を与えて、音波の伝播を詳細に計算し、翼端渦や音波の定性的な値は実験と一致していることを確認した。

キーワード：乱流、DNS、コルモゴロフスケール、LES、翼、騒音、翼端渦

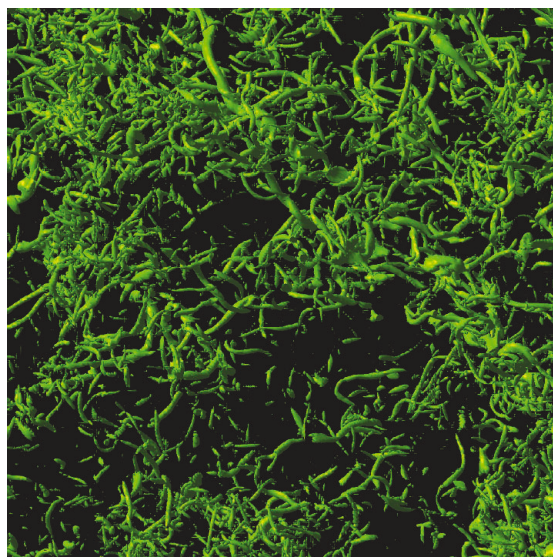


図1 一様減衰乱流場の可視化